

Research on Synthesis of FeCo@N-C and Activation Persulfate

Jun Chen^{1,*}, Shangqing Xia¹, Longchi Zhao¹, Sisi Cao¹, Cheng Zong¹, and Jie Jin¹

¹Hefei University, School of Biology, Food and Environment, Anhui Key Laboratory of Sewage Purification and Eco-restoration Materials, 230601, Hefei, Anhui, China

Abstract. Based on the characteristics of persulfate (PS) activation that can quickly and effectively remove organic pollutants in water, a new catalytic material of carbon nitride supported Fe-Co diatom (FeCo@N-C) was prepared for PS activation to degrade orange II (OII). The XRD pattern showed that eight characteristic diffraction peaks, including CoFe_2O_4 diffraction absorption peaks. The FT-IR inferred that C-N/C=N, C=O, and O-H functional groups may exist. SEM observed the surface morphology of the synthetic material, and Fe and Co can be successfully loaded on the synthetic material. The activation effect of FeCo@N-C activator on PS was significantly improved, and the decoloration removal rate reached 81.66% at 20 min, 57% higher than the PS alone, FeCo@N-C activator had a good pH and temperature adaptability. FeCo@N-C activator could promoted the production of free radicals which can degrade OII efficiently.

1 Introduction

Advanced Oxidation Process (AOPs) can directly mineralize high concentration organic wastewater with poor biodegradability and high relative molecular weight or improve the biochemical properties of pollutants through oxidation, and can completely mineralize or decompose most organic compounds, which has a good application prospect [1-2]. Orange II (OII) is a typical anionic azo dye. Due to its advantages of brilliant color, stable coloring and low price, OII is widely used in the dyeing of various textiles [3]. However, OII aqueous solution has a high salt content, which will have a serious impact on the activities of aquatic organisms when release into water. Therefore, OII was selected as the degradation target. The degradation of OII was carried out by the activation of persulfate (PS) and the main active oxide was $\text{SO}_4^{\cdot-}$. Compared with AOPs with ($\cdot\text{OH}$) as the main active substance, the activation process of AOPs base on PS is suitable for a wide pH range, still has a higher active site under alkaline conditions, and the half-life is longer than that of single activation, which is conducive to the long-term degradation of the target pollutant OII [4-5]. Transition metals can be activated efficiently at ambient temperature, such as Ag, Cu, Fe, Co, Mn and other transition metal ions. In addition to the transition metal for PS activation, there are also non-transition metal materials for PS activation, and the most used is carbon materials. Carbon material itself uses natural advantages, such as large specific surface area, large pores, low economic cost, no worries about secondary pollution, and good stability [6]. We can neutralize two catalytic pathways, so that transition metal ions can be loaded onto carbon-based materials. Two or more active groups could improve the activation efficiency of PS. Based on the characteristics of PS activation that can quickly and effectively remove organic pollutants in water [7], a new

catalytic material carbon nitride supported Fe-Co diatom (FeCo@N-C) catalyst was prepared for PS activation, the synergistic catalysis of Fe and Co had also been reported [8-9]. The coprecipitation pyrolysis method was used to prepare FeCo@N-C material, nitrogen doping graphene also exhibited excellent catalytic performance because doping N could endow the high binding energy with PS, which enhances electrontransfer from graphene to PS [10-12], and during this process XRD was used. FT-IR, SEM, and other means could intuitively observe the surface morphology of the material.

2 Materials preparation and methods

2.1 Experimental reagents and instruments

Iron nitrate nonahydrate ($\text{Fe}(\text{NO}_3)_3 \cdot 9\text{H}_2\text{O}$) were purchased from Sinopharm Chemical Reagent Co.LTD. Cobalt-nitrate hexahydrate ($\text{Co}(\text{NO}_3)_2 \cdot 6\text{H}_2\text{O}$) were purchased from Tianjin Bodi Chemical Co., LTD.absolute methanol(CH_3OH), hydrochloric acid,sodium hydroxidewere purchased from Xilong Scientific Co., Ltd.PS ($\text{K}_2\text{S}_2\text{O}_8$) were purchased from Unixide Initiator Shanghai Co., LTD. Carbamide ($\text{CO}(\text{NH}_2)_2$) was purchased from Tianjin Damao Chemical Reagent Factory. Tropeolin($\text{C}_{16}\text{H}_{11}\text{N}_2\text{NaO}_4\text{S}$), melamine ($\text{C}_3\text{H}_6\text{N}_6$) were purchased from Shanghai Maclean Biochemical Technology Co., LTD. The water used in the whole study was deionized. All above chemicals and reagents were of analytically pure without further purification.

* Corresponding author: chenjun@hfuu.edu.cn

2.2 Synthesis of FeCo@N-C

The preparation of FeCo@N-C was completed by precipitation and carbonization, and the specific steps were as follows.

2.2.1 Preparation of precursor

0.202 g of $\text{Fe}(\text{NO}_3)_3 \cdot 9\text{H}_2\text{O}$, 0.145 g of $\text{Co}(\text{NO}_3)_2 \cdot 6\text{H}_2\text{O}$ and 3.003 g of urea put them into an agate mortar (during the synthesis process, the total amount of iron nitrate 9 hydrate and cobalt nitrate hexahydrate was 1 mmol, and the ratio of metal salt to urea was 30-100. In this experiment, the production ratio was 100), and 10 mL anhydrous ethanol was added to fully grind for 30min to obtain reddish-brown solute. The solid obtained was dried at 60 °C for 6 h in an air blast drying oven, which was the precursor [13].

2.2.2 Preparation of catalyst

Before pouring the obtained precursor into the crucible, it was best to grind it into uniform powder, and then set the heating program (3 °C/min-5 °C/min) to heat up to 800 °C for high-temperature carbonization for 2 h, and then naturally cool to room temperature to took out black solid, namely FeCo@N-C [14]. concentration was respectively arranged. Using pure water as a reference, a quartz cuvette with the optical path of 10mm was used to measure its absorbance at a wavelength of 484 nm, and the standard curve was prepared.

2.3 Experimental steps for degrading dye wastewater

Took 10 mL of OII dye waste from the standard reserve solution into a 100 mL volumetric flask and dilute it with pure water to the scale line to obtain 100 mg/L OII dye waste. Repeat this step three times to obtain three 100 mL 100 mg/L OII dye waste. Took three 150 mL conical bottles. Pour the required reagents and materials into the conical flask from the volumetric flask, and oscillate in a 25 °C constant temperature oscillator (100 rpm) for 5 min, 10 min, 15 min, 20 min, 25 min, and 30 min. Then, used a 5 mL disposable syringe to absorb 3 mL of dye waste liquid and filter it with a 0.45 um disposable needle filter. A small amount of anhydrous methanol was added to stop the reaction. Then the absorbance was measured at wavelength 484 nm [15], and the concentration was calculated by using the standard curve, and then the removal rate was calculated. The decoloration efficiency was calculated by the following formula:

$$W = (C_0 - C_e) / C_0 \times 100\% \quad (1)$$

Where W was decoloration efficiency

C_0 was the initial concentration of OII dye waste liquid (mg/L)

C_e was the instantaneous concentration of OII dye waste liquid (mg/L)

2.4 Analytical methods

TD-3500 X-ray diffractometer (Dandong Tongda) was employed to radiate the sample to obtain their X-ray diffraction (XRD) patterns. The functional groups on the surface of the sample was analyzed by Fourier transform infrared spectrophotometer (FT-IR, Nicolet 6700, America), and the spectra was recorded in the range of 4000 to 1000 cm^{-1} . The SEM spectra of the sample was observed by SU8010 cold field emission scanning electron microscope (Thermo Fisher Scientific, USA).

3 Results and discussions

3.1 characterization and physicochemical characteristics analysis of FeCo@N-C

To determine the main components of the synthetic material, the material was characterized by XRD. Jade software was used to retrieve the physical phase of the material, and then the data were derived and processed to obtain the graph shown in Fig. 1 (a). The figure above was the XRD pattern of FeCo@N-C in the range of 2θ 20-80°. It can intuitively see the characteristic diffraction peaks of CoFe_2O_4 at $2\theta=30.1^\circ, 35.5^\circ, 43.1^\circ, 57.0^\circ, \text{ and } 62.8^\circ$, according to the standard JCPDS (card # 22-1086), indicating that Fe and Co were successfully combined on N-C.

The absorption spectrum after data processing was shown in Fig. 1 (b). In the infrared spectrum, the wavelength or wave-number position of the absorbed light will form absorption peaks. According to this characteristic, some functional groups in the synthetic material can be viewed. $\text{C}=\text{O}$ at 1735 cm^{-1} and possible O-H at 2930 cm^{-1} .

To intuitively observe the synthetic materials and prove that iron and cobalt were successfully loaded on the surface of carbon nitride, SEM was used to observe FeCo@N-C at different multiples. The SEM spectrum of the sample was shown in Fig. 1 (c). The overall shape of carbon nitride material was flake with microspores, it can be observed that there were many Fe and Co granular objects attached to N-C material, which were spherical.

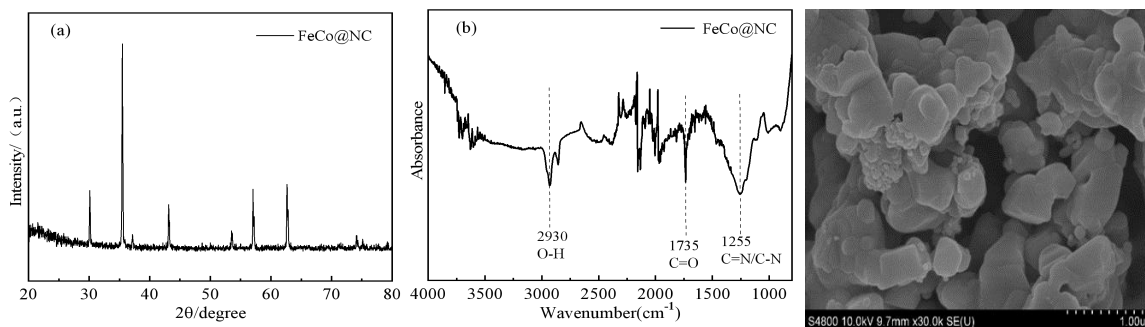


Fig. 1. (a) XRD patterns, (b) FT-IR spectra, (c) SEM spectra of FeCo@N-C.

3.2 Study on the degradation efficiency and influencing factors of OII by FeCo@N-C activation PS

3.2.1 Study on degradation efficiency of OII by FeCo@N-C activation PS

Under the initial experimental conditions of the same temperature, pH and initial concentration of OII, took 3 150 mL conical bottles, took 100 mL 100 mg/L OII dye waste liquid, added 0.05 g FeCo@N-C, 2 g PS, 0.05 g FeCo@N-C and 2 g PS, respectively. Oscillate in a 25°C thermostatic oscillator (100 rpm), the absorbance was measured, and the concentration was calculated using the standard curve, and then the removal rate was calculated. The experimental results were shown in Fig. 2.

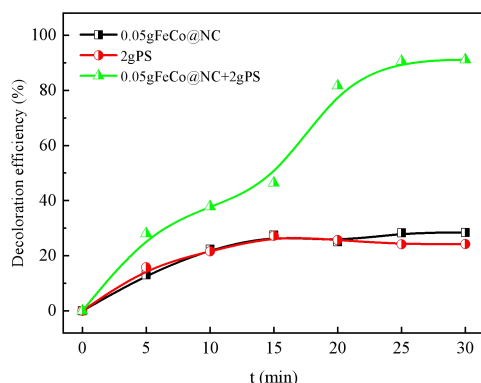


Fig. 2. Effect of catalyst on degradation of OII

As can be seen from Fig. 2, when FeCo@N-C prepared in the experiment was put in alone, it could not remove OII well, and the removal rate was 28.41% after 30 min. When PS was added alone, the reaction was slow due to the low activity of PS itself, and the removal rate was only 24.25% at 30 min. However, when PS was activated by the catalyst, the discoloration removal rate reached 81.66% at 20 min, showed a good catalytic effect. The decolorization efficiency of PS activated by Fe and Co alone on carbon nitride was 50.32% and 63.67% in 20 min, respectively, which was lower than that activated by FeCo@N-C.

3.2.2 FeCo@N-C Influence of dosage

Under the premise of the same initial concentration of OII, pH, temperature, and PS dosage, took 3 150 mL conical bottles, took 100 mL 100 mg/L OII dye waste liquid, add 2 g PS, and press FeCo@N-C of 0.5 g/L, 1.0 g/L, and 1.5 g/L, respectively. Oscillate in a 25°C thermostatic oscillator (100 rpm), the absorbance was measured, and the concentration was calculated using the standard curve, and then the removal rate was calculated. At the same time, the influence of FeCo@N-C dosage on catalytic PS was studied. The experimental results were shown in Fig. 3.

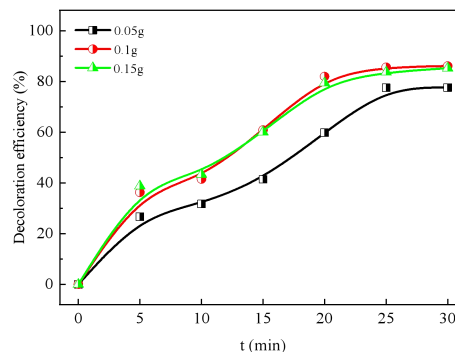


Fig. 3. Effect of FeCo@N-C dosage on degradation of OII

According to Fig. 3, the addition amount of FeCo@N-C to catalytic potassium PS was slightly lower in the case of 0.5 g/L, while there was no significant difference in case of 1 g/L and 1.5 g/L. However, compared with 0.5 g/L, the experimental results showed that the instantaneous removal rate of OII could be accelerated with the increase of the additional amount, indicated that the loaded bimetallic atom sites on the material were relatively uniform. Its catalytic efficiency could achieve the optimal effect at 1 g/L and finally tends to balance.

3.2.3 Effect of initial pH of reaction on the degradation of OII

OII was a weak acid substance, and the initial pH of 100 mg/L OII simulated dye waste liquid prepared

was 5.56. Take 4 150 mL conical bottles, and take 100 mL 100 mg/L OII dye waste liquid. The pH was adjusted to 3, 5, 7, and 10 with 0.1 mol/L HCl and NaOH, then 0.05 g sludge-based activated carbon and 2 g PS was added. Oscillate in a 25°C thermostatic oscillator (100 rpm) and took samples every 5 min for 6 times in total, the absorbance was measured. Use the standard curve to calculate the concentration, and then calculate the removal rate. The effect of the initial pH of solution on catalytic PS was analyzed. The experimental results were shown in Fig. 4.

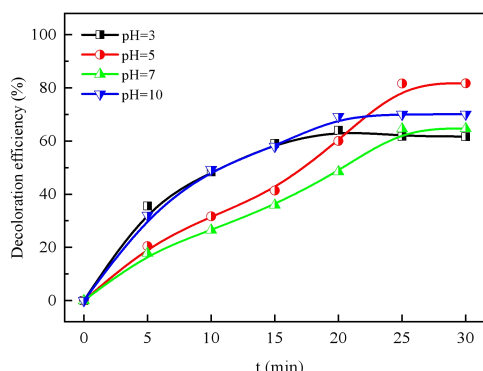


Fig. 4. Effect of different pH on degradation of OII

The pH value of the reaction solution has an important influence on the types of free radicals generated in advanced oxidation technology and the degradation of organic pollutants. After adding PS to the conical flask, the pH value was adjusted to 3, 5, 7, 10. Fig. 4 showed that OII had a better degradation effect under weak acid conditions. The final removal rate of 3, 7, and 10 fluctuates little, indicating that the material was adaptable to a wide range of pH and the higher the pH was, the more negative charge on the surface of FeCo@N-C. OII was an anionic material, resulting in electrostatic inhibition, so the pH of 10 was weaker than that of 5. When the pH of the reaction solution was 3, the degradation rate of OII was slower than that of pH 5, which may be due to the formation of hydrogen bond between H⁺ and O-O bond in PS under strongly acidic conditions, which led to the reduction of PS activation efficiency as well as the degradation rate [16].

3.2.4 Influence of temperature on degradation of OII

Took three 150 mL conical bottles, added 100 mL of 100 mg/L OII dye waste liquid, then added 0.5 g FeCo@N-C and 2 g PS, in a thermostatic oscillator (100 rpm), the oscillations were carried out at 10°C, 25°C and 40°C, respectively, and samples were taken every 5 min for a total of 6 times, the absorbance was measured. The concentration was calculated using the standard curve, and the removal rate was calculated. The result was shown in Fig. 5.

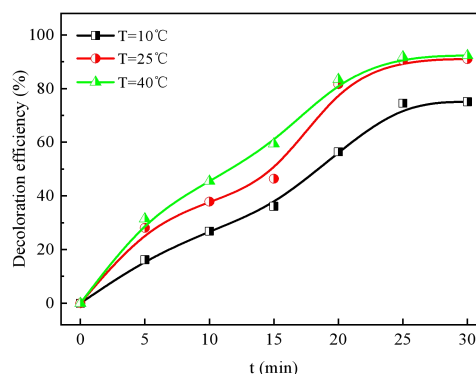


Fig. 5. Effect of temperature on degradation of OII

Fig. 5 illustrated the: reaction to 10 min, the removal rate increased with the increase of temperature was small, the removal rate of the OII small-amplitude increases with the increase of the temperature quickly, this may be due to the increase of the temperature, thus speeding up the intermolecular Brownian motion, accelerating the oxide free radical generation, so as to speed up the degradation rate [17]. However, there was no significant difference between 25 °C and 40 °C (the removal rate reached 81.66% and 83.45% respectively at 25 min), indicating that temperature had little overall influence on the experimental effect [18]. Considering practical factors, 25 °C was the optimal temperature for this experiment.

3.3 Mechanism and kinetics of degradation of OII by FeCo@N-C activation PS

3.3.1 Kinetic simulation of degradation of OII by FeCo@N-C activated PS

The reaction kinetics of the chemical reaction in the degradation process of OII was analyzed and the reaction rate constant was obtained. The kinetic analysis of the degradation of OII by activated PS was a complex process. The quasi-first-order kinetic equation and pseudo-second-order kinetic equation were used to linearly fit the dosage of different FeCo@N-C materials. The following was the dynamic model.

Quasi-first-order dynamics model was:

$$-\ln(C_0 / C) = K_1 t \quad (2)$$

Pseudo-second-order dynamics model was:

$$(1/C - 1/C_0) = K_2 t \quad (3)$$

Where C was the instantaneous concentration of OII at time;

C₀ was the initial concentration of OII;

K₁ quasi-first-order reaction rate constant (min⁻¹);

K₂ was pseudo-second-order reaction rate constant (min⁻¹);

t was degradation time;

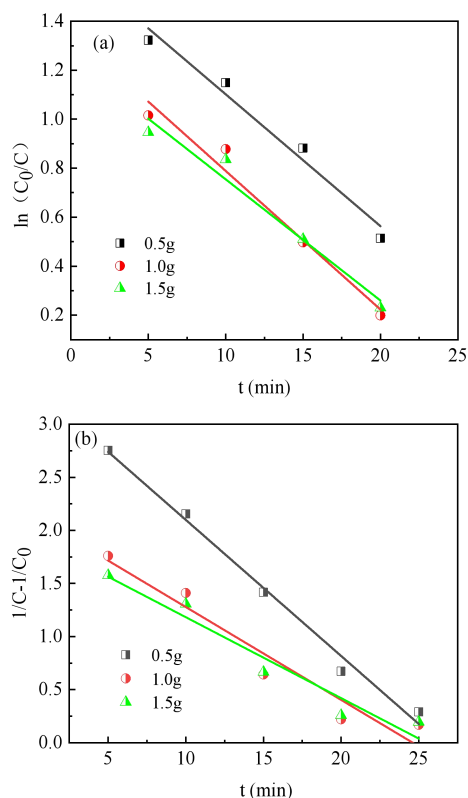


Fig. 6. (a) Quasi-first-order kinetic curves of degradation of OII with different FeCo@N-C dosage, (b) Pseudo-second-order kinetic curves of OII degradation with different FeCo@N-C dosage.

As can be seen from Fig. 6 (a) and 6 (b), degradation processes of OII under different FeCo@N-C dosage were in line with quasi-first-order dynamic model and pseudo-second-order dynamic model. When FeCo@N-C dosage was 0.5 g, 1.0 g and 1.5 g, respectively, the corresponding first-order reaction rate constant (K_1) and second-order reaction rate constant (K_2) were -0.05383, -0.05658 and -0.04949, respectively. -0.12818, -0.08749, -0.07624. It can be seen that as the dosage increases, the slope increases, which means the reaction rate accelerates. According to the analysis, this was because the increase of material dosage, the removal of OII reaction system has more active sites, more active groups, the activation of PS produced more free radicals, which led to a faster degradation rate.

3.3.2 Mechanism of activation of PS by FeCo@N-C

Took three 100 mL 100 mg/L OII dye waste liquid into conical bottles, added 0.5 g FeCo@N-C and 2 g PS into three conical bottles, and add 40mL methanol (MeOH) and 40mL tert-butanol (TBA) to two of them respectively to quench reactive oxygen species (ROS). Oscillate in a 25°C thermostatic oscillator (100 rpm), the absorbance was measured, and the concentration was calculated using the standard curve, and then the removal rate was calculated.

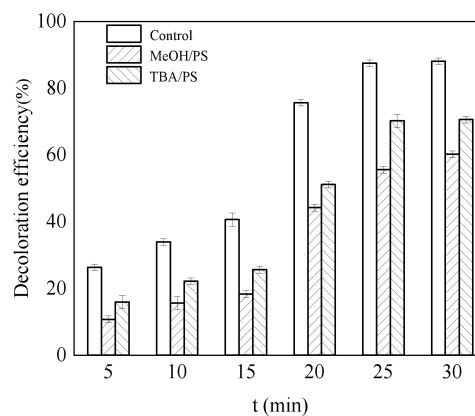
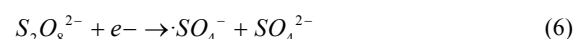
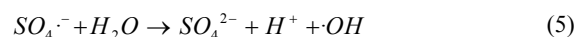
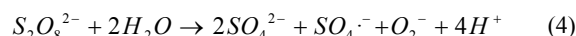


Fig. 7. Influence of MeOH and TBA quenching

Under the same temperature and pH, MeOH and TBA, two quenching agents, were selected to identify ROS involved in degradation of OII. As shown in the Fig. 7, when MeOH was added to quench $SO_4^{\cdot-}$, $\cdot OH$ and 1O_2 the degradation efficiency of OII was significantly reduced, indicating that $SO_4^{\cdot-}$, $\cdot OH$ and 1O_2 played a role, but after the addition of TBA, it only decreased by about 10%. TBA alcohol mainly quenches $\cdot OH$, but the effect was not obvious, indicating that the degradation effect of $SO_4^{\cdot-}$, 1O_2 on OII was greater than that of $\cdot OH$.

The activation mechanism was mainly divided into the following aspects, the responsible ROS for OII degradation in PS/FeCo@N-C system were $SO_4^{\cdot-}$, $\cdot OH$ and 1O_2 . The reaction between PS ion and water produced $SO_4^{\cdot-}$, $\cdot OH$ and 1O_2 . The prepared catalyst contained Fe and Co ions, which could activate metal PS to produce $SO_4^{\cdot-}$, and the material of non-metallic catalyst itself has a certain activation performance to PS. The mechanism was expressed in the following chemical equation in order:



4 Conclusion

FeCo@N-C was synthesized to activate PS and decompose OII., and the degradation rate of 81.66% can be achieved in 20 min. The experimental results showed that this material had a certain effect on PS activation. The dosage of FeCo@N-C for degradation of OII accorded with the quasi-first order kinetic model and pseudo second order kinetic model. The reaction mechanism was the reaction of PS ions with water to produced $SO_4^{\cdot-}$, $\cdot OH$ and 1O_2 . $SO_4^{\cdot-}$ plays a major role in activation. The prepared catalyst contained Fe and Co ions, which could activate metal PS to produced $SO_4^{\cdot-}$. N-doped carbon shells could provided a large number of active sites for PS activation, the material of non-metallic catalyst itself had certain activation performance to PS. FeCo@N-C activated PS to produced free radicals that rapidly

destroyed the chromophile groups of OII. This led to the fading of OII

This research was supported by the National Key R&D Program of China (2020YFC1908601, 2020YFC1908602). Hefei University graduate innovation and entrepreneurship program. Science Development Fund Project of Hefei University (22040521004).

References

1. M. Rayaroth, C. Aravindakumar, N. Shah, et al. Advanced oxidation processes (AOPs) based wastewater treatment-unexpected nitration side reactions-a serious environmental issue: A review. *J. Chemical Engineering Journal*: 133002 (2021).
2. Y. Deng, R. Zhao. Advanced Oxidation Processes (AOPs) in Wastewater Treatment. *J. Current Pollution Reports*, **1(3)**:167-176 (2015).
3. Y. Liu, K. Yan, S. Xue, A review on dyeing wastewater treatment. *J. Textile Dyeing and Finishing Journal*, **36(07)**:8-12 (2014).
4. X. Gu, Y. Wang, Z. Miao, et al. Degradation of trichloroethylene in aqueous solution by persulfate activated with Fe(III)-EDDS complex. *J. Research on Chemical Intermediates*, 43(1):1-13 (2017).
5. D. Ge, Y. Zhu, G. Li, et al. Identifying the key sludge properties characteristics in Fe²⁺-activated persulfate conditioning for dewaterability amelioration and engineering implementation. *J. Journal of environmental management*, 296: 113204 (2021).
6. Y. Gao, Q. Wang, G. Ji, et al. Degradation of antibiotic pollutants by persulfate activated with various carbon materials. *J. Chemical Engineering Journal*: 132387 (2021).
7. Q. Xu. The Degradation of Methyl Orange by SodiumPersulfate with Co-loaded Activated Carbon as Catalyst. *J. Chemical Engineering & Equipment*, **(11)**:11-15 (2016).
8. X. Gu, Y. Ji, J. Tian, et al. Combined MOF derivation and fluorination imparted efficient synergism of Fe-Co fluoride for oxygen evolution reaction. *J. Chemical Engineering Journal*, **427**: 131576 (2022).
9. G. Huang, C. Wang, C. Yang, et al. Degradation of bisphenol A by peroxymonosulfate catalytically activated with Mn_{1.8}Fe_{1.2}O₄ nanospheres: synergism between Mn and Fe. *J. Environmental science & technology*, **51(21)**: 12611-12618 (2017).
10. X. Duan, Z. Ao, H. Sun, et al. Nitrogen-doped graphene for generation and evolution of reactive radicals by metal-free catalysis. *J. ACS applied materials & interfaces*, **7(7)**: 4169-4178 (2015).
11. P. Duan, T. Ma, Y. Yue, et al. Fe/Mn nanoparticles encapsulated in nitrogen-doped carbon nanotubes as a peroxymonosulfate activator for acetamiprid degradation. *J. Environmental Science: Nano*, **6(6)**: 1799-1811 (2019).
12. H. Sun, X. Peng, S. Zhang, et al. Activation of peroxymonosulfate by nitrogen-functionalized sludge carbon for efficient degradation of organic pollutants in water. *J. Bioresource Technology*:244-251 (2017).
13. W. Nan, Y. Lei, Q. Wang, et al. Facile synthesis of FeCo@N-C core-shell nanospheres supported on graphene as an efficient bifunctional oxygen electrocatalyst. *J. Nano Research*, **10(7)**:2332-2343 (2017).
14. P. Duan, Y. Qi, S. Feng, et al. Enhanced degradation of clothianidin in peroxymonosulfate/catalyst system via core-shell FeMn@N-C and phosphate surrounding. *J. Applied Catalysis B: Environmental*, **267**: 118717 (2020).
15. B. Zhu, H. Cheng, J. Ma, et al. Bi₂MoO₆ microspheres for the degradation of orange II by heterogeneous activation of persulfate under visible light. *J. Materials Letters*, **261**: 127099 (2020).
16. G. Wang, S. Chen, X. Quan, et al. Enhanced activation of peroxymonosulfate by nitrogen doped porous carbon for effective removal of organic pollutants. *J. Carbon*, **15**:730-739 (2017).
17. C. Cai, J. Liu, Z. Zhang, et al. Visible light enhanced heterogeneous photo-degradation of Orange II by zinc ferrite (ZnFe₂O₄) catalyst with the assistance of persulfate. *J. Separation and Purification Technology*, **165**:42-52 (2016).
18. Y. Kuang, J. Du, R. Zhou, et al. Calcium alginate encapsulated Ni/Fe nanoparticles beads for simultaneous removal of Cu (II) and monochlorobenzene. *J. Journal of Colloid and Interface Science*, **447**:85-9 (2015)